J Mater Sci: Mater Electron (2017) 28:3140–3150
DOI 10.1007/s10854-016-5902-6

Synthesis and studies on effect of indium doping on physical properties of electrodeposited CdSe thin films

Vanita S. Raut[1] · Chandrakant D. Lokhande[2] · Vilas V. Killedar[1]

Received: 31 August 2016 / Accepted: 15 October 2016 / Published online: 20 October 2016

Abstract Semiconducting CdSe and indium doped CdSe (In: CdSe) thin films have been synthesized on stainless steel and fluorine doped tin oxide coated glass substrates in an aqueous medium using a potentiostatic mode of electrodeposition. The doping concentration of indium has been optimized to 0.15 vol% using the reliable photoelectrochemical technique. To study the effect of indium doping these films are characterized using X-ray diffraction, X-ray photoelectron spectroscopy (XPS), field emission scanning electron microscopy, energy dispersive X-ray spectroscopy, elemental mapping, Raman spectroscopy, contact angle measurement and UV–visible spectrophotometry techniques. CdSe and In: CdSe thin films are low crystalline with a cubic crystal structure. The valence states of CdSe and In: CdSe thin films are analyzed by means of XPS. Undoped CdSe thin film shows fiberlike morphology, which transforms into a beautiful web of nanofibers upon doping. The Elemental composition of both films analyzed by means of energy dispersive X-ray spectroscopy. Raman studies show transverse optical and longitudinal optical modes of phonon. Indium doping improves the hydrophilic nature of CdSe photoanode. The optical band gap (direct) found to be decreased from 2.02 to 1.67 eV upon indium doping. Both films are photoactive in nature.

✉ Vilas V. Killedar
killedar_vilas@yahoo.co.in

[1] Department of Physics, Rajarshi Chhatrapati Shahu College, Kolhapur, MH 416003, India

[2] Thin Film Physics Laboratory, Department of Physics, Shivaji University, Kolhapur, MH 416004, India

1 Introduction

From last few decades, a study of various semiconductors has attracted a grand deal of attention for its wide range of applications. Researchers have been trying to alter the physical and chemical properties of various semiconductor materials using different techniques to further explore their potential. Doping is one of the effective ways to alter the optical, electrical as well as the magnetic properties of semiconductor materials [1, 2]. Momeni et al. [3–11] doped titanium dioxide and tungsten trioxide—titanium dioxide photoanodes with chromium, cobalt, copper, gold, iron, and manganese. They found that, doped photoanodes show enhanced performance in photocatalysis and solar water splitting application, which is attributed to modification in band gap energy by the introduction of dopant energy states, thus shifting optical response from ultra-violet to the visible region. Especially in photoelectrochemical (PEC) cell lower performance of photoanode is attributed to higher values of band gap and electrical resistivity that could be efficiently reduced by doping it with suitable impurity. Among various II–VI semiconductors, Cadmium Selenide (CdSe) is a one of the most versatile photoanode material with band gap (1.7 eV) near to visible spectrum maxima. It has earned recognizable attention of researchers because of the high absorption coefficient, direct band gap, size dependant physical and chemical properties, intrinsic birefringence and luminescent properties. These properties promote use of CdSe in various applications as solar cell [12–14], thin film transistor [15], light emitting diode [16] and various electronic devices [17] etc. CdSe thin films have been grown by diverse physical and chemical techniques such as thermal evaporation [18], hot wall deposition [19], electron beam evaporation [20], chemical bath deposition [21, 22], electrodeposition [23], spray pyrolysis

[24], hydrothermal [25], successive ionic layer adsorption and reaction [26] methods etc.

The performance of the CdSe thin film has been enhanced in various applications via doping it with suitable dopant materials. Ali and El-Ghanny [27] have grown indium, zinc and tin doped CdSe thin films on glass substrate by electron beam evaporation technique. They reported, indium doped cadmium selenide film (In: CdSe) shows the lowest value of resistivity. Perna et al. [28] doped indium in CdSe lattice by laser ablation technique. They observed bandgap narrowing and band tails in absorption spectra upon indium doping. Mahalingam et al. [29] electrodeposited In: CdSe thin films. They reported improvement in crystallinity, decrease in band gap (from 1.7 to 1.63 eV), strain and dislocation density corresponding to doping with 0.02 mM indium concentration. Hankare et al. [30] deposited indium doped $Cd_{0.9}Zn_{0.1}Se$ thin films by chemical bath deposition method. They reported superior PEC cell performance corresponding to 0.1 mol% indium doping. Yadav [31] has deposited indium doped $CdS_{0.2}Se_{0.8}$ thin film by spray pyrolysis technique. He found superior PEC performance for 0.15 mol% indium doped $CdS_{0.2}Se_{0.8}$ thin film ($\eta = 2.12$ %, FF = 0.49) than pristine ($\eta = 0.79$ %, FF = 0.46).

As doping with trivalent indium is found to enhance electrical conductivity, decrease the band gap and also to improve performance of PEC cell significantly, thus we have chosen indium as a dopant in the synthesis of CdSe thin films. Amongst the various deposition techniques, electrodeposition is simple, economic and low cost technique. By this technique, films can be grown over a large area with high scalability, without vacuum and at room temperature [32]. Thus electrodeposition technique was selected for thin film deposition purpose.

The aim of the current study is to synthesize indium doped CdSe thin film by facile electrodeposition technique for photoanode purpose. Thus to inspect the influence of volumetric indium doping on physical properties of CdSe thin film and to discuss its results.

2 Experimental details

2.1 Deposition of CdSe and In: CdSe thin films

Thin film synthesis was carried out using a three electrode cell with graphite bar (60 mm × 13 mm × 4 mm) as a counter electrode, saturated calomel electrode (SCE) as a reference electrode and substrate as a working electrode. Potentiostatic electrosynthesis of CdSe and In: CdSe thin films was carried out on fluorine doped tin oxide (FTO) coated glass substrates and stainless steel substrates using a scanning potentiostat of Princeton applied research company.

Substrate cleaning plays very vital role in the deposition process. Therefore prior to deposition, FTO coated glass substrates (sheet resistance of 15–20 Ω cm^{-2}) were boiled in chromic acid and ultrasonically cleaned. Stainless steel substrates (50 mm × 10 mm × 0.5 mm) were mirror polished by zero grade polish paper, cleaned with liquid detergent labogene, etched in 5 % H_2SO_4 for 5 min and finally ultrasonically cleaned.

All the chemicals used for synthesis ($3CdSO_4{\cdot}8H_2O$, SeO_2 and $InCl_3$) were analytical reagent grade. Double distilled water was used for preparation of all precursor solutions. With the intention to obtain more photosensitive electrodeposit, a PEC method is used to optimize preparative parameters of CdSe thin film. In PEC method, the photosensitivity of samples [short circuit current (J_{sc}) and open circuit voltage (V_{oc})] is checked so as to choose better photosensitive sample [33]. For this purpose, the PEC cell was fabricated using two electrode configuration, with CdSe as photoanode and graphite as counter electrode. 1 M polysulfide (1 M NaOH–1 M Na_2S–1 M S) was used as redox electrolyte. The performance of PEC cell was studied under illumination intensity 50 mW/cm^2. The area of photoanode exposed to light was 1 cm^2 other than that was enclosed by insulating tape to prevent any other contribution to the net photocurrent density. A PEC solar cell was fabricated in an airtight system by just direct dipping the CdSe or In: CdSe photoanode in polysulfide electrolyte, so as to keep away oxygen from redox electrolyte.

2.1.1 *Deposition of CdSe thin film and optimization of preparative parameters by PEC method*

During preparation of CdSe thin film, initially the selenium concentration varied from 0.1 to 0.0005 M keeping the cadmium concentration fixed to 0.05 M. Figure 1a shows variation in J_{sc} and V_{oc} as a function of selenium concentration at fixed cadmium concentration (0.05 M). It is seen that values of J_{sc} and V_{oc} increase with the decrease in Selenium concentration and attain maximum value at 0.01 M selenium concentration corresponding to Cd:Se concentration ratio is 5:1. For further decrease in concentration of selenium both J_{sc} and V_{oc} drops. This may be due to stoichiometric CdSe formation taking place at 5:1 Cd:Se concentration ratio [34]. At other selenium precursor concentration deviation from stoichiometry taking place.

Polarization curves were recorded using linear sweep voltammetry technique for these optimized concentrations using a scanning potentiostat for Cd, Se and undoped CdSe thin films from their respective baths. The potential was scanned from 0 to −1 V/SCE with a scan rate 20 mV/s. The polarization curves for Cd, Se and undoped CdSe (on

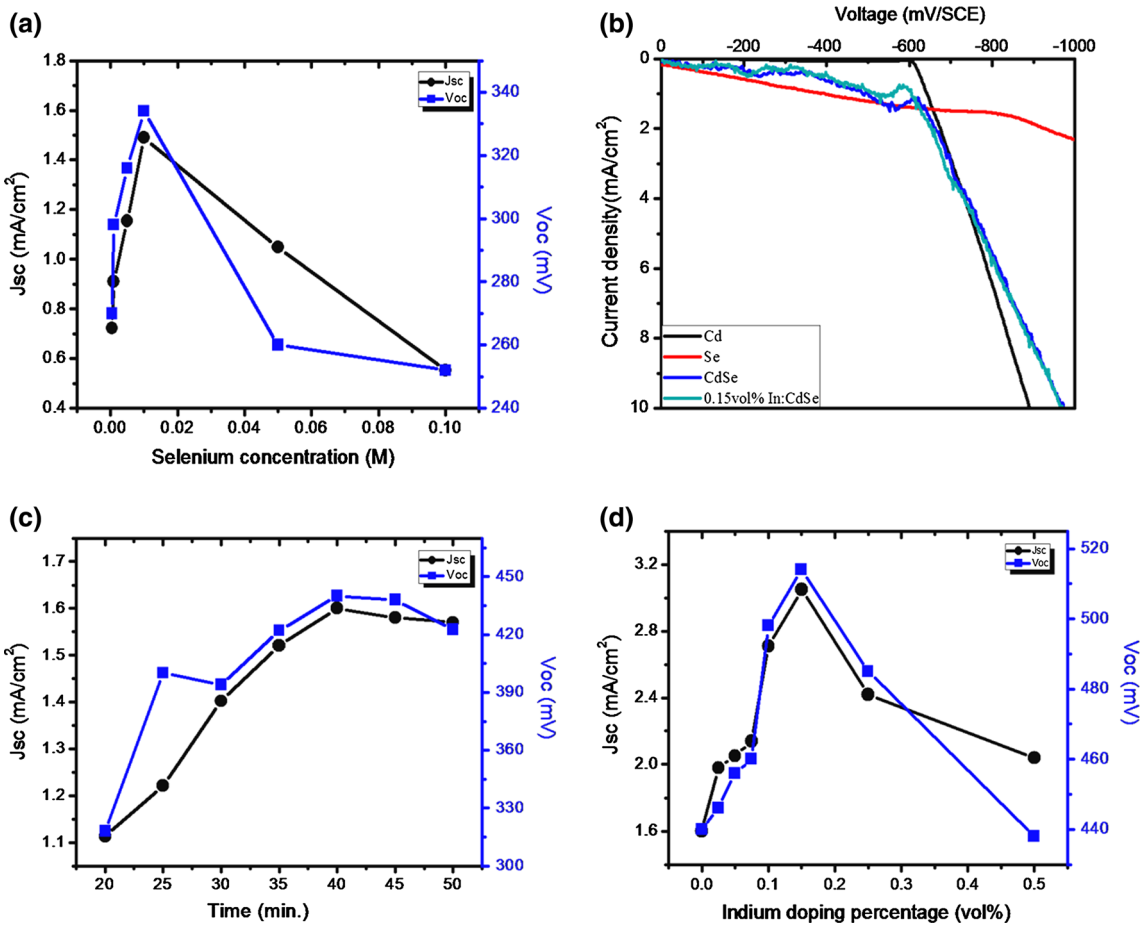

Fig. 1 **a** Variation of J_{sc} and V_{oc} with selenium concentration for CdSe/1 M Polysulfide/C PEC cell, **b** cathodic polarization curves for Cd, Se, CdSe and 0.15 vol% In: CdSe thin films on stainless steel substrate, **c** variation of J_{sc} and V_{oc} with deposition time for CdSe/1 M Polysulfide/C PEC cell and **d** variation of J_{sc} and V_{oc} with volumetric indium doping percentage

substrate area 1.5 cm^2, at pH = 3) are plotted to estimate deposition potentials are shown in Fig. 1b (polarization curve for 0.15 vol% In: CdSe is also included in Fig. 2) All potentials were measured with respect to Saturated Calomel Electrode (SCE). The potential corresponding to the point of intersection of the tangent on potential axis represents the reduction potential. The estimated deposition potentials obtained from polarization curves are listed in the Table 1. It reveals that the deposition potential of CdSe lies among reduction potential of cadmium and selenium [35]. The CdSe thin film of brown color was found to be deposited at deposition potential −590(±10) mV/SCE. Room temperature electrodeposition of CdSe thin films was carried out by employing a potentiostatic mode at −590 mV/SCE from the electrolytic bath (pH = 3) containing 0.05 M $CdSO_4$ and 0.01 M SeO_2 in 1:1 proportion.

Deposition time was optimized using PEC method. Figure 1c shows variation in J_{sc} and V_{oc} as a function of deposition time. The values of J_{sc} and V_{oc} are found to be maximum corresponding to deposition period 40 min, which are attributed to maximum film thickness 490 nm attained by CdSe thin film. For further increase in deposition time both J_{sc} and V_{oc} decreases. After 40 min film starts to redissolve in the bath.

2.1.2 *Deposition of In: CdSe thin films*

For deposition of indium doped cadmium selenide (In: CdSe) thin films an indium trichloride ($InCl_3$) was used as source material. The doping percentage of indium was varied by adding appropriate volume of 0.05 M $InCl_3$ solution to electrodeposition bath using micropipette so as to maintain volumetric doping percentage 0.025, 0.050, 0.075, 0.1, 0.15, 0.25 and 0.5. For indium doping percentage higher than 0.5 vol%, electrolyte bath becomes turbid, milky precipitate settles down in the bath which constrains film formation. pH of bath maintained to 3 using dilute H_2SO_4. All In: CdSe thin films were deposited without aid of any complexing agent. The doping percentage of indium was optimized using PEC method. The variation in J_{sc} and V_{oc} with indium volumetric doping percentage is shown in Fig. 1d. It is found that J_{sc} and V_{oc}

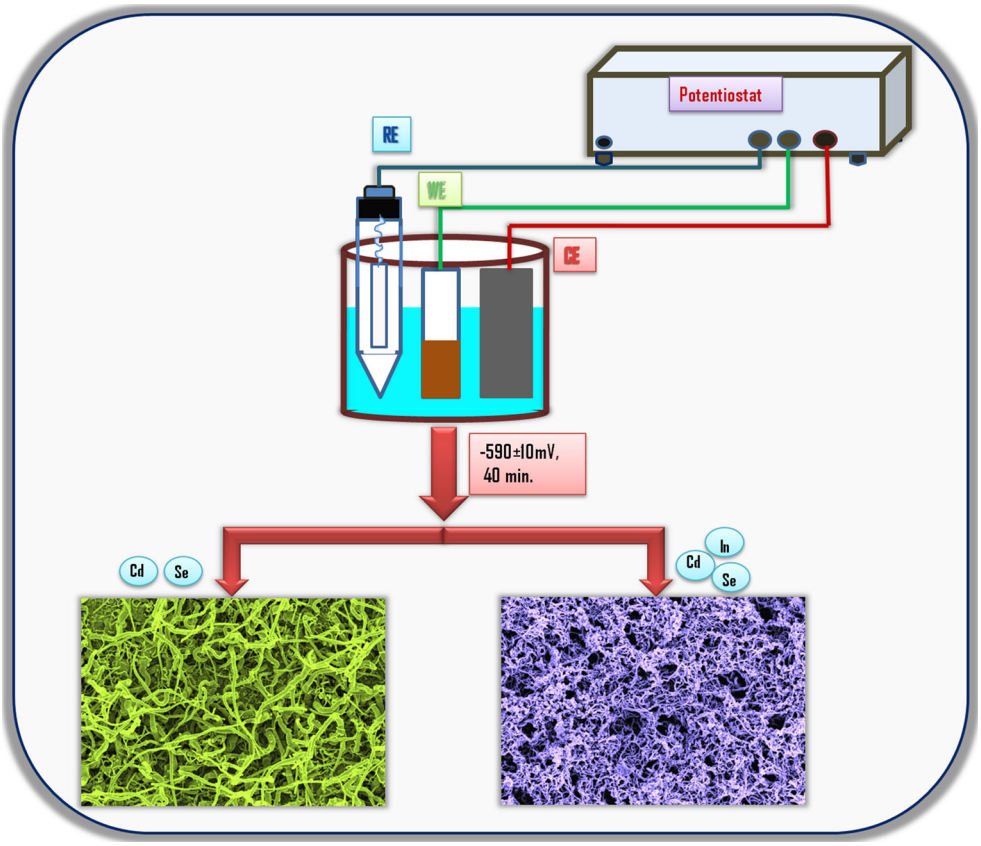

Fig. 2 A schematic representation of electrodeposition set up for synthesis of undoped and indium doped CdSe samples

Table 1 Estimated deposition potentials for Cd, Se, undoped CdSe and 0.15 vol% In: CdSe thin films for stainless steel substrate

Sample	Cd	Se	CdSe	0.15 vol% In: CdSe
Deposition potential (mV/SCE)	−610	−470	−590	−580

both increases with increase in indium doping percentage, reaches maximum values corresponding to 0.15 vol% doping percentage and then drop off for further increase in indium doping percentage. This drop off in J_{sc} and V_{oc} may be due to stoichiometric deviation and increased resistivity of In: CdSe thin films [36]. The optimized doping percentage of indium in CdSe thin film found to be 0.15 vol%. The cathodic polarization curve for 0.15 vol% In: CdSe thin film is shown in Fig. 1b. A careful look at this figure shows that, deposition of In: CdSe film occurs at more positive potential than CdSe. It may be due reduction potential of indium is less cathodic than cadmium [37]. As no significant difference observed in the deposition potential of CdSe and 0.15 vol% In: CdSe thin films as in Table 1. Thus, both films deposited under same optimized preparative conditions and used for further studies. A schematic representation of synthesis of undoped and indium doped CdSe thin films using electrodeposition technique is shown in Fig. 2.

2.2 Characterizations

The structural investigation of the films was carried out by using Philips X-ray diffractometer PW-3710. The source of radiation was Cu Kα with $\lambda = 1.54$ Å. The 2θ was varied between range 10°–100°. The analysis of elemental information was made using an X-ray photoelectron spectroscopy (HR-XPS, VG Multilab 2000, Thermo VG scientific and UK). A surface morphological study and energy dispersive X-ray analysis was carried out by JEOL-JSM 6360 unit. Raman spectra were recorded, with a Jobin Yvon Horibra LABRAM-HR visible spectrometer with an argon-ion continuous-wave laser of wavelength 488 nm as an excitation source, for confirmation of CdSe phase. The thickness of deposited samples was measured with Ambios XP-1 surface profiler. The contact angle measurement was carried out to study the interaction between the liquid and thin film electrode surface by Rame-Hart USA equipment equipped with a CCD camera. The optical absorption study

was carried out using a UV spectrophotometer UV-1800 SHIMADZU in a wavelength range 300–900 nm with FTO coated glass substrate.

3 Results and discussion

3.1 X-ray diffraction (XRD) studies

XRD patterns of undoped CdSe and 0.15 vol% In: CdSe thin film are shown in Fig. 3. The comparison of the observed XRD patterns with Standard JCPDS data (card no. 00-019-0191) confirms the formation of CdSe with a cubic crystal structure. Both CdSe and In: CdSe thin films are amorphous in nature with broad humps observed in XRD patterns. The diffraction peaks observed close to 2θ values 25.24° and 82.36° are indexed to (111) (511) planes of cubic CdSe respectively, which are in good agreement with nanocrystalline CdSe thin films electrodeposited by Sarangi and Sahu [38]. No any separate peak observed for indium, CdO or SeOx. The peaks marked as SS correspond substrate contribution which might be owing to low thickness of film or interference from XRD signals of stainless steel substrate. The XRD pattern shows, (with indium doping) decrease in broadening of (111) peak which enhances its intensity. The (111) diffraction peak becomes more intense and narrower corresponding to 0.15 vol% Indium doped CdSe thin film, indicating improvement in quality of the electrodeposit which may be responsible for enhancement of photovoltaic performance of the same.

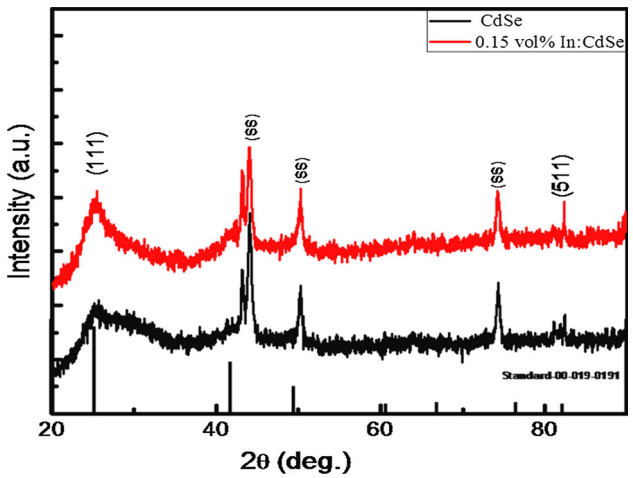

Fig. 3 X-ray diffraction pattern of potentiostatically electrodeposited undoped CdSe and 0.15 vol% In: CdSe thin films. *Vertical lines at bottom* show standard JCPDS peaks (card no. 00-019-0191) of a cubic phase

3.2 X-ray photoelectron spectroscopy (XPS) studies

The valence states of undoped CdSe and 0.15 vol% In: CdSe thin films are confirmed by X-ray photoelectron spectroscopy (XPS). The survey spectrum signifies presence of Cadmium (Cd), Selenium (Se), Indium (In) and C. The carbon is probably due to capping agents and the contamination as a consequence of sample contact to the environment. The 3d core level spectra for all constituents Cd, Se and In are shown in Fig. 4. The upper panel of Fig. 4 shows the XPS spectra of undoped CdSe thin film, in which narrow scan spectra for Cd and Se species are designated as (a) and (b) respectively. While the lower panel of Fig. 4 shows the XPS spectra of 0.15 vol% In: CdSe thin film containing narrow scan spectra for Cd, Se and In designated as (a′), (b′) and (c′) respectively.

The Cd 3d core level spectra split into two peaks observed at 412.07 and 405.31 eV ascribed to Cd $3d_{3/2}$ and Cd $3d_{5/2}$ respectively (Fig. 4a) and are in close agreement with earlier reports in the literature [39–41] suggesting that the cadmium valence state in the CdSe is +2. These two peaks are separated by energy difference 6.76 eV well matches with the earlier reports [42, 43]. In Se 3d core level spectrum, the position of binding energy maxima occurs at 54.27 eV. The deconvolution of the spectrum gives two peaks at 54.99 and 54.13 eV separated by energy difference 0.86 eV. These peaks are corresponds to Se $3d_{3/2}$ and Se $3d_{5/2}$ (Fig. 4b) respectively, suggesting that the selenium present in valence state −2 [42, 44]. The Cd and Se peak locations shift jointly. The binding energy difference between two peak positions is 351.18 ± 0.1. For bulk CdSe it is 350.97 eV [41]. This result evidently reveals that CdSe material has been successfully synthesized.

The Cd 3d XPS spectra for 0.15 vol% In: CdSe thin film (Fig. 4a′) show two peaks located at binding energies of 412.19 and 405.45 eV corresponds to the Cd $3d3_{/2}$ and Cd $3d5_{/2}$ core levels of Cd^{2+} cation. The energy separation between these peaks is 6.74 eV found to be decreased and is in close agreement with earlier report [43]. Doping process replaces one cation with other cation. This replacement results in decrease in binding energy for doped samples than undoped one [45]. The Se 3d XPS spectrum for 0.15 vol% In: CdSe sample (Fig. 4b′) shows peak maxima at 54.33 eV, deconvolution of it gives two peaks located at binding energies of 54.75 and 53.86 eV corresponding to the Se $3d3_{/2}$ and Se $3d5_{/2}$ core levels of Se^{2-} anion respectively. The energy separation between these two peaks found to be increased to 0.89 eV. The In 3d XPS spectra for 0.15 vol% In: CdSe thin film (Fig. 4c′) show two peaks located at binding energies of 452.83 and 445.20 eV corresponding to the In $3d3_{/2}$ and In $3d5_{/2}$ core levels of In^{3+} cation respectively. The energy separation between these peaks is found to be 7.63 eV. These values

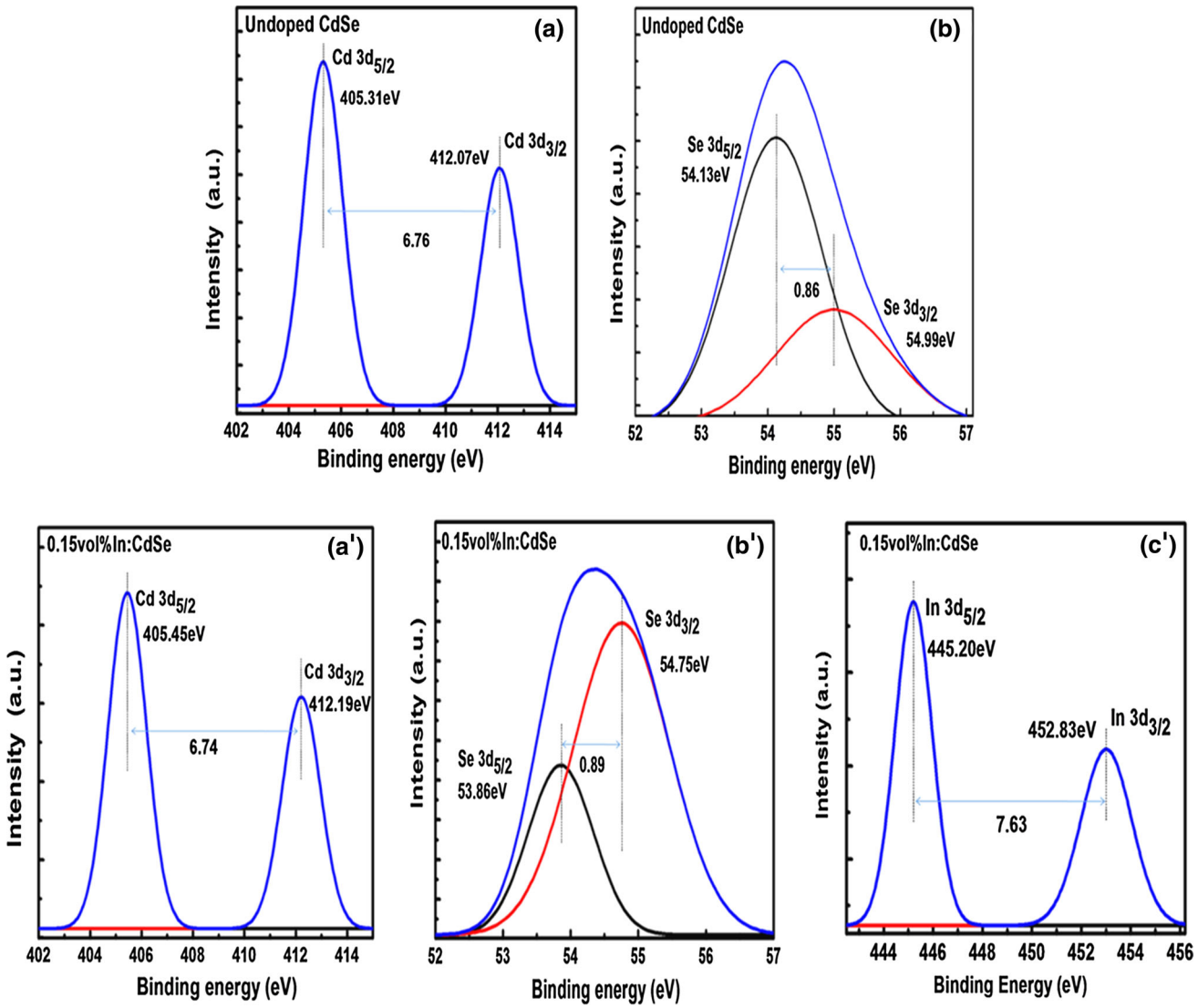

Fig. 4 The narrow scan XPS spectra for cadmium and selenium of pure CdSe thin film (upper panel) designated as (**a**) and (**b**) respectively. The narrow scan XPS spectra for cadmium, selenium and indium of 0.15 vol% In: CdSe (lower panel) thin film designated as (**a**′), (**b**′) and (**c**′) respectively

are in close agreement with earlier report [46]. Binding energy values obtained from XPS analysis matches well with earlier reports and this manifest presence of indium in CdSe lattice confirms the successful synthesis of In: Cdse thin films. Binding energy values obtained from XPS analysis for Cd, Se and In elements of pure CdSe and 0.15 vol% In: CdSe thin films are summarized in Table 2.

3.3 Morphological and compositional studies

The morphological modulation induced in CdSe thin film via indium doping was studied using FESEM. Morphology plays significant role in enhancing performance of a particular application. FESEM images of undoped CdSe and 0.15 vol% In: CdSe thin films at lower (1 μm—5KX) and higher (1 μm—10KX) magnification are shown in Fig. 5.

Table 2 Binding Energy values obtained from XPS spectra analysis for pure CdSe and 0.15 vol% In: CdSe samples

Sample	Binding energy (eV)						
	Cd $3d_{5/2}$	Cd $3d_{3/2}$	Se 3d	Se $3d_{5/2}$	Se $3d_{3/2}$	In $3d_{5/2}$	In $3d_{3/2}$
Undoped CdSe	405.31	412.07	54.27	54.13	54.99	Nil	Nil
0.15 vol% In: CdSe	405.45	412.19	54.33	53.86	54.75	445.20	452.83

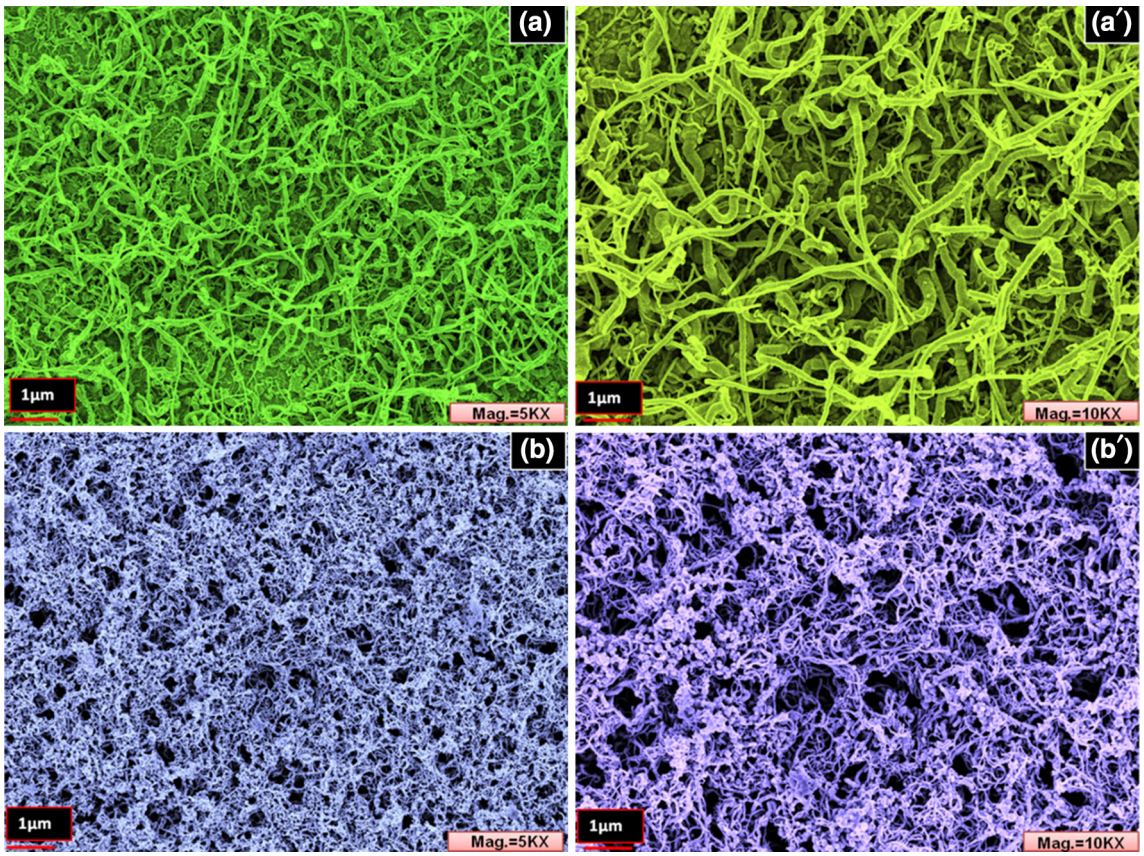

Fig. 5 FESEM images of undoped CdSe and 0.15 vol% In: CdSe thin films at lower (**a**, **b**) and higher (**a′**, **b′**) magnification respectively

Undoped CdSe thin film shows fiberlike morphology. Web like interconnected fibers of diameter ranging between 50 and 150 nm and length from 4 to 7 µm are found to be dispersed all over the substrate. The lower and higher magnification FESEM image of the undoped CdSe thin film is shown in Fig. 5a, a′ respectively. Min et al. [47] reported analogous morphology for galvanostatically electrodeposited CdSe thin films grown on ITO substrate. Further indium doping shows significant modulation in morphology. FE-SEM image of 0.15 vol% In: CdSe thin film shows a compact and crowded web of interconnected nanofibers with marvelously bloomed buds like structure on it. Such type of morphology is extremely useful for solar cell applications as it provides better capturing of photon and electrode electrolyte contact. The lower and higher magnification FESEM image of 0.15 vol% In: CdSe thin film is shown in Fig. 5b, b′ respectively.

The elemental composition of the undoped CdSe and 0.15 vol% In: CdSe sample was studied using energy-dispersive X-ray spectroscopy (EDX). EDX patterns for undoped and doped CdSe samples are presented in Fig. 6a, b respectively. Figure 6a shows CdSe sample mainly consisted of Cd and Se while Fig. 6b clearly shows presence of indium along with Cd and Se in a doped sample. The particulars of atomic percentage analysis of undoped and doped CdSe samples are given in Table 3, which shows that undoped CdSe samples are slightly cadmium rich. It also authenticates the incorporation of indium in the doped CdSe sample. The spatial distribution of constituent elements on the surface of undoped CdSe and In: CdSe samples was studied by EDX mapping. The results are displayed in Fig. 6c, d. The elemental maps demonstrate distribution of Cd, Se and In on the surface of the undoped and doped sample.

3.4 Raman spectroscopy studies

The Raman spectra of electrodeposited CdSe and 0.15 vol% In: CdSe thin films recorded in the range 0–400 cm^{-1} is shown in Fig. 7. The Raman spectrum of CdSe thin film exhibits 3 peaks with bands at 169.14, 209.42 and 251.97 cm^{-1}. The weak band in the spectrum at about 209.42 cm^{-1} is ascribed to longitudinal optical (LO) phonon mode of CdSe. The bulk CdSe shows LO phonon mode at 210 cm^{-1}. The red Shift observed in LO phonon mode is effect of phonon confinement [48]. The peak observed at around 169.14 cm^{-1} is attributed to transverse optical (TO) phonons. The band at 252.15 cm^{-1} is

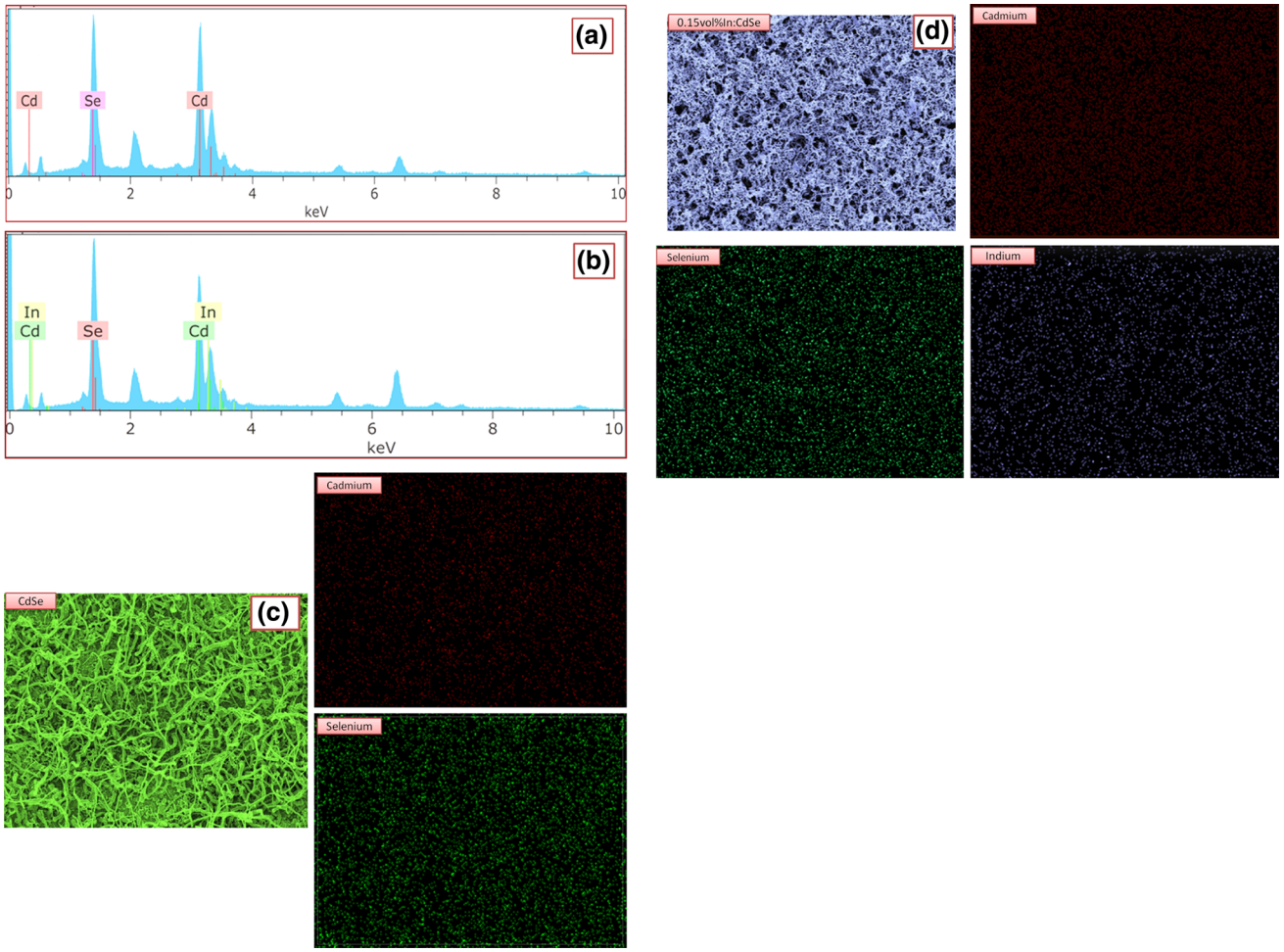

Fig. 6 EDX patterns of **a** undoped CdSe, **b** 0.15 vol% In: CdSe sample. Elemental EDX mapping of **c** undoped CdSe and **d** 0.15 vol% In: CdSe, indicating the spatial distribution of Cd, Se and In on the surface of samples

Table 3 Elemental compositional of undoped CdSe and In: CdSe thin films obtained from EDX analysis

Sample	Atomic percentage of element		
	Cd	Se	In
Undoped CdSe	55.53	44.47	–
0.15 vol% In: CdSe	54.89	43.81	1.30

assigned to out of phase Cd–Se–Cd modes [49]. These bands found to be shifted towards slightly higher frequencies at 171.44, 209.52, 252.15 cm^{-1} for 0.15 vol% In: CdSe thin film which may be due to incorporation on indium ions in CdSe lattice [50]. The Raman shift values for CdSe and 0.15 vol% In: CdSe thin films have been listed in Table 4.

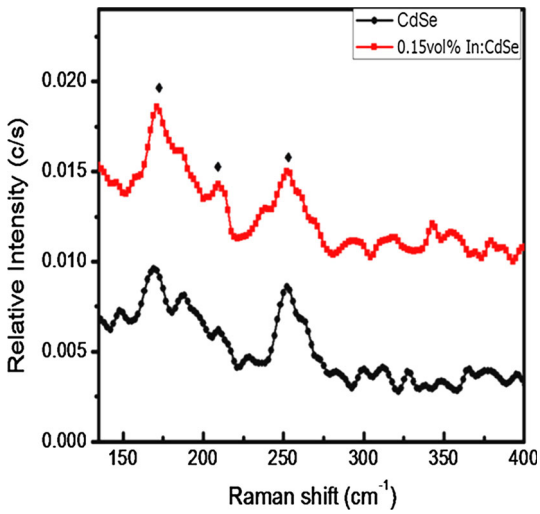

Fig. 7 Raman spectra of undoped CdSe and 0.15 vol% In: CdSe thin films at room temperature. *Filled diamond* indicates the peak position

Table 4 Raman shift values for CdSe and 0.15 vol% In: CdSe thin films

Sample Modes	Undoped CdSe Position (cm^{-1})	0.15 vol% In: CdSe Position (cm^{-1})
Transverse optical	169.14	171.44
Longitudinal optical	209.42	209.52
Cd–Se–Cd	251.97	252.15

3.5 Thickness and wettability studies

Figure 8 displays variation in film thickness for undoped CdSe and 0.15 vol% In: CdSe thin film. Film thickness of doped sample is found to be greater than pure CdSe thin film. Increased film thickness enlarges the width of depletion region which avails more area for photon absorption, thus resulting in enhancement of PEC performance for the same.

Wettability study discusses the interaction between CdSe or In: CdSe electrode with electrolyte which is described by value of contact angle. Water contact angle measurement images for undoped CdSe and 0.15 vol% In: CdSe thin films are shown in Fig. 8. The water contact angle values for CdSe and 0.15 vol% In: CdSe thin film found to be 58° and 37.8° respectively. This decrease in water contact angle is attributed to increase in surface roughness upon indium doping. Smaller the contact angle more is the hydrophilic nature of electrode surface which results into intimate contact between photoanode and redox electrolyte in solar cell. A smaller contact angle of 0.15 vol% In: CdSe electrode makes it more suitable for solar cell application than pristine CdSe [51].

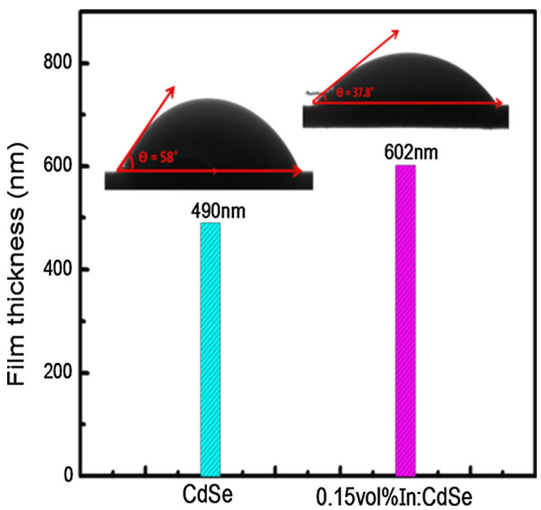

Fig. 8 Variation in film thickness and contact angle for undoped CdSe and 0.15 vol% In: CdSe thin film

3.6 Optical absorbance and band gap studies

Optical properties of the material play a very crucial role in various device performances. The optical absorption spectra of pristine and 0.15 vol% In: CdSe thin film was recorded at room temperature using UV–visible spectrophotometer in the wavelength range 350–850 nm. The band gap energy was estimated from the plot of $(\alpha h\upsilon)^{\wedge}2$ versus $h\upsilon$ by extrapolating a tangent on energy axis. Intercept of a tangent on the energy axis for zero absorption coefficient provides band gap energy value. In semiconductors for near edge optical absorption, the analysis of optical absorption data was made by classical relation.

$$\alpha = \frac{\alpha_0(h\upsilon - Eg)^{\wedge}n}{h\upsilon} \quad (1)$$

where α_0 is a constant, $h\upsilon$ is photon energy, E_g is the band gap energy, n is a constant

n = 1/2, 3/2, 2 and 3 for direct allowed, direct forbidden, indirect allowed and indirect forbidden transitions respectively [52].

Figure 9 shows a plot of $(\alpha h\upsilon)^{\wedge}2$ versus $h\upsilon$ for undoped CdSe (marked as A) and 0.15 vol% In: CdSe (marked as B) thin film. Inset displays optical absorption spectra for the same. The linear nature of $(\alpha h\upsilon)^{\wedge}2$ versus $h\upsilon$ plots indicates presence of direct transition for both pristine CdSe and 0.15 vol% In: CdSe semiconducting material. The band gap energy found to be 2.02 eV for pure CdSe, which further decreases to minimum value 1.67 eV corresponding to indium doping percentage 0.15 vol%. This result can be explained as undoped CdSe is a n-type semiconductor whose source is credited to selenium vacancies. In CdSe, selenium vacancy acts as donor center and cadmium vacancy act as an acceptor center. Excess cadmium in

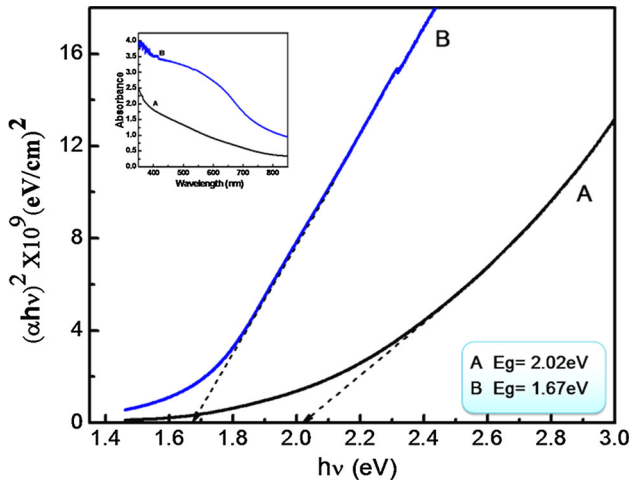

Fig. 9 Band gap plots of undoped CdSe (*designated as A*) and 0.15 vol% In: CdSe (*designated as B*) thin films. *Inset* shows absorbance spectra

CdSe creates donor levels in the band gap region. For sufficiently high cadmium concentration (i.e. n-CdSe) these donor levels become degenerate and merge into the conduction band, thus increasing absorbance for pure CdSe. Further addition of trivalent indium creates donor levels in the band gap region near the conduction band which decreases the band gap. Closer the Fermi level to the conduction band, the higher is the concentration of majority carriers that is electrons. Band gap reduction shifts absorption edge to longer wavelength side increasing optical absorbance (as shown in Fig. 9). Thus more portion of the solar energy spectrum can be utilized [53, 54]. 0.15 vol% In: CdSe thin film shows red shift in absorbance with superior performance than undoped CdSe.

4 Conclusions

The synthesis of undoped and indium doped CdSe thin films is possible using facile potentiostatic electrodeposition technique. The superior PEC performance is observed corresponding to indium doping percentage 0.15 vol%. Indium doping found to be induced structural, optical and morphological modulations in CdSe thin film. Both CdSe and 0.15 vol% In: CdSe thin films are found to be low crystalline in nature with a cubic crystal structure. Intensity of (111) plane is improved upon indium doping. The XPS analysis of CdSe and In: CdSe thin films clears presence of cadmium, selenium and indium in valence states $+2$, -2 and $+3$ respectively. The XPS analysis confirmed successful synthesis of CdSe and In: CdSe thin films. A beautiful morphological modulation observed from CdSe fibers to bloomed bud like structure grown on web of interconnected nanofibers corresponding to 0.15 vol% Indium doping. EDX and elemental EDX mapping analysis showed that indium is incorporated in the doped CdSe sample and sample is composed of Cd, Se and In. Contact angle measurements showed smaller contact angle consequently more hydrophilic nature for indium doped CdSe thin film than pristine. The band gap energy found to be decreased from 2.02 to 1.67 eV upon indium doping.

Acknowledgments One of the authors (VSR) is grateful to University Grants Commission, New Delhi for the award of teacher fellowship and thankful to the Secretary, Rayat Shikshan Sanstha, Satara for granting the study leave. VSR also wish to acknowledge Mr. Abhishek Lokhande and Dr. Nilesh Chodankar for the valuable discussion.

References

1. C.X. Xu, X.W. Sun, X.H. Zhang, L. Ke, S.J. Chua, Nanotechnology **15**, 856 (2004)
2. J. Sivasankar, P. Mallikarjana, M.R. Begam, N.M. Rao, S. Kaleemulla, J. Subrahmanyam, J. Mater. Sci. Mater. Electron. **27**, 2300 (2016)
3. M.M. Momeni, Y. Ghayeb, Z. Ghonchegi, Surf. Eng. **32**, 520 (2016)
4. M.M. Momeni, Y. Ghayeb, J. Solid State Electrochem. **20**, 683 (2016)
5. M.M. Momeni, Y. Ghayeb, J. Mater. Sci. Mater. Electron. **27**, 3318 (2016)
6. M.M. Momeni, I. Ahadzadeh, Mater. Res. Innov. **20**, 44 (2016)
7. M.M. Momeni, Y. Ghayeb, Z. Ghonchegi, Ceram. Int. **41**, 8735 (2015)
8. M.M. Momeni, Y. Ghayeb, Appl. Phys. A **122**, 620 (2016)
9. M.M. Momeni, Y. Ghayeb, J. Electroanal. Chem. **751**, 43 (2015)
10. M.M. Momeni, Mater. Res. Innov. **20**, 317 (2016)
11. M.M. Momeni, M. Hakimian, A. Kazempour, Surf. Eng. **32**, 514 (2016)
12. R.B. Kale, C.D. Lokhande, Appl. Surf. Sci. **223**, 343 (2003)
13. H. Wynands, M. Cocivera, Chem. Mater. **3**, 143 (1991)
14. S.J. Lade, M.D. Uplane, C.D. Lokhande, Mater. Chem. Phys. **68**, 36 (2001)
15. A. Vancalster, A. Vervaet, I. Derycke, J. Dedaets, J. Vanfleteren, J. Cryst. Growth **86**, 924 (1988)
16. V.L. Colvin, M.C. Schlamp, A.P. Allvlsatos, Nature **370**, 354 (1994)
17. O.I. Olusola, O.K. Echendu, I.M. Dharmadasa, J. Mater. Sci. Mater. Electron. **26**, 1066 (2015)
18. C. Baban, G.I. Rusu, Appl. Surf. Sci. **211**, 6 (2003)
19. S. Velumani, X. Mathew, P.J. Sebastian, S.K. Narayandass, D. Mangalaraj, Sol. Energy Mater. Sol. Cells **76**, 347 (2003)
20. S. Mathuri, K. Ramamurthi, R.R. Babu, J. Mater. Sci. Mater. Electron. **27**, 7582 (2016)
21. C.D. Lokhande, E.-H. Lee, K.-D. Jung, O.-S. Joo, Mater. Chem. Phys. **91**, 200 (2005)
22. H.M. Gubur, F. Septekin, S. Alpdogan, B. Sahan, B.K. Zeyrek, J. Mater. Sci. Mater. Electron. **27**, 7640 (2016)
23. G. Hodes, I.D.J. Howell, L.M. Peter, J. Electrochem. Soc. **139**, 11 (1992)
24. R.K. Beri, P.K. Khanna, V. Singh, B.R. Mehta, Curr. Appl. Phys. **11**, 809 (2011)
25. Q. Peng, Y. Dong, Z. Deng, Y. Li, Inorg. Chem. **41**, 5249 (2002)
26. H.M. Pathan, B.R. Sankapal, J.D. Desai, C.D. Lokhande, Mater. Chem. Phys. **78**, 11 (2002)
27. H.M. Ali, H.A.A. El-Ghanny, J. Phys. Condens. Matter **20**, 155205 (2008)
28. G. Perna, V. Capozzi, A. Minafra, M. Pallara, M. Ambrico, Eur. Phys. J. B **32**, 339 (2003)
29. T. Mahalingam, R. Mariappan, V. Dhanasekaran, S.M. Mohan, G. Ravi, J.P. Chu, Chalcogenide Lett. **7**, 669 (2010)
30. P.P. Hankare, P.A. Chate, D.J. Sathe, Phys. B **404**, 2389 (2009)
31. A.A. Yadav, J. Mater. Sci. Mater. Electron. **27**, 4508 (2016)
32. R.K. Pandey, S.N. Sahu, S. Chandra, *Handbook of Semiconductor Electrodeposition* (Marcel Dekker, Inc, New York, 1996), p. 2
33. S.M. Pawar, A.V. Moholkar, K.Y. Rajpure, C.H. Bhosale, J. Phys. Chem. Solids **67**, 2386 (2006)
34. K. Bieńkowski, M. Strawski, B. Maranowski, M. Szklarczyk, Electrochim. Acta **55**, 8908 (2010)
35. N.S. Yesugade, C.D. Lokhande, C.H. Bhosale, Thin Solid Films **263**, 145 (1995)
36. A.A. Yadav, E.U. Masumdar, Mater. Res. Bull. **45**, 1445 (2010)
37. R.K. Pandey, S.N. Sahu, S. Chandra, *Handbook of Semiconductor Electrodeposition* (Marcel Dekker, Inc, New York, 1996), Appendix 1, p. 252
38. S.N. Sarangi, S.N. Sahu, Phys. E **23**, 159 (2004)
39. Z. Chen, W. Peng, K. Zhang, J. Zhang, X. Yang, Y. Numata, L. Han, J. Mater. Chem. A **2**, 7004 (2014)

40. N. Winograd, S.W. Gaarenstroom, X-ray photoelectron spectroscopy. Phys. Methods Mod. Chem. Anal. **2**, 164. (http://www.psu.edu/dept/winograd/pdf/70.pdf)
41. J.E.B. Katari, V.L. Colvin, A.P. Alivisatos, J. Phys. Chem. **98**, 4109 (1994)
42. J.W. Kim, H.S. Shim, S.W. Ko, U. Jeong, C.L. Lee, W.B. Kim, J. Mater. Chem. **22**, 20889 (2012)
43. S.A. Pawar, D.S. Patil, S.K. Patil, D.V. Awale, R.S. Devan, Y.-R. Ma, S.S. Kolekar, J.-H. Kim, P.S. Patil, Electrochim. Acta **148**, 310 (2014)
44. E. Agostinelli, C. Battistooni, D. Fiorani, G. Mattogno, M. Noguess, J. Phys. Chem. Solids **50**, 269 (1989)
45. M. Venkata-Haritha, C.V.V.M. Gopi, C.V. Tulasi-Varma, S.-K. Kim, H.-J. Kim, J. Photochem. Photobiol. A **315**, 34 (2016)
46. H. Chen, S.M. Yu, D.W. Shin, J.B. Yoo, Nanoscale Res. Lett. **5**, 217 (2010)
47. S.-K. Min, O.-S. Joo, R.S. Mane, K.-D. Jung, C.D. Lokhande, S.-H. Han, J. Photochem. Photobiol. A **187**, 133 (2007)
48. V.M. Dzhagan, M.Y. Valakh, A.E. Raevskaya, A.L. Stroyuk, S.Y. Kuchmiy, D.R.T. Zahn, Nanotechnology **19**, 305707 (2008)
49. S. Wageh, Phys. E **39**, 8 (2007)
50. S. Das, A. Dutta, S. Banerjee, T.P. Sinha, Mater. Sci. Semicond. Process. **18**, 152 (2014)
51. S.K. Shinde, D.P. Dubal, G.S. Ghodake, V.J. Fulari, RSC Adv. **4**, 33184 (2014)
52. V.V. Killedar, S.N. Katore, C.H. Bhosale, Mater. Chem. Phys. **64**, 166 (2000)
53. C.D. Lokhande, S.H. Pawar, Solid State Commun. **44**, 1137 (1982)
54. A.A. Yadav, M.A. Barote, T.V. Chavan, E.U. Masumdar, J. Alloys Compd. **509**, 916 (2011)